Journal of Photochemistry & Photobiology, B: Biology 191 (2019) 150–155

Contents lists available at ScienceDirect

Journal of Photochemistry & Photobiology, B: Biology

journal homepage: www.elsevier.com/locate/jphotobiol

Green synthesis of multi-color emissive carbon dots from *Manilkara zapota* fruits for bioimaging of bacterial and fungal cells

Jigna R. Bhamore[a], Sanjay Jha[b], Tae Jung Park[c], Suresh Kumar Kailasa[a,*]

[a] Department of Applied Chemistry, S. V. National Institute of Technology, Surat 395 007, India
[b] Gujarat Agricultural Biotechnology Institute, Navsari Agricultural University, Surat 395007, India
[c] Department of Chemistry, Institute of Interdisciplinary Convergence Research, Research Institute of Halal Industrialization Technology, Chung-Ang University, 84 Heukseok-ro, Dongjak-gu, Seoul 06974, Republic of Korea

ARTICLE INFO

Keywords:
Fluorescent C-dots
Manilkara zapota fruits
Multi-color emission
Bioimaging

ABSTRACT

Natural resources have widely been used as precursors for the preparation of ultra-small carbon dots (C-dots) due to ease of availability, low cost and C-dots with high quantum yields (QYs). Herein, water dispersible multi-color emissive C-dots were obtained from *Manilkara zapota fruits*. The emission of C-dots was well tuned by sulphuric acid and phosphoric acids, which results to generate blue-, green- and yellow- C-dots. The fabricated C-dots exhibit blue, green and yellow color emissions when irradiated them under UV light at 365 nm. The emission/excitation peaks of blue-, green-, and yellow- C-dots were observed at 443, 515 and 563 nm when excited at 350, 420 and 440 nm, respectively. The QYs of blue-, green-, and yellow- C-dots are 5.7, 7.9 and 5.2%. The average sizes of blue- green- and yellow- C-dots are 1.9 ± 0.3, 2.9 ± 0.7and 4.5 ± 1.25 nm, respectively. Because of ultra-small size and biocompatibility, three C-dots act as promising bioimaging agents for imaging of cells (*E. coli*, *Aspergillus aculeatus* and *Fomitopsis* sp). The cytotoxicity on HeLa cells indicates that three C-dots have non-toxic nature, which confirms their biocompatibility. The ultra-small C-dots were effectively distributed in the cytoplasm of the cells, ensuring the potential applications in cell imaging and biomedical studies.

1. Introduction

Due to their unique optical properties and surface functional groups, ultra-small C-dots have been used as potential fluorescent probes in various applications including sensing, drug delivery and cell imaging [1]. Since C-dots have strong and excitation depended photoluminescence (PL) properties, which make them as excellent candidates in biomedical, chemical and bio-sensing and catalytic applications [2–6]. Further, C-dots are functionalized with biomolecules for drug delivery and for bioimaging applications. Importantly, ultra-small C-dots have effectively replaced semiconductor quantum dots (QDs) because of their easy preparation, multi-color emission, high quantum yield (QY) and biocompatibility [7–9].

Generally, ultra-small C-dots are synthesized by using various molecules as precursors (organic, biomolecules, natural resources and polymeric and waste materials) [10,11]. To make them as potential fluorescent materials with unique surface functionalities, several synthetic approaches including arc discharge [12], microwave [13], pyrolysis [14–17], hydrothermal [18] and laser ablation [10,11] methods have been widely used for the generation of ultra-small fluorescent C-dots. Among these synthetic approaches, the carbonization of natural resources (plant materials) in the presence of acids has received significant interest due to the generation of different fluorescent colors of ultra-small C-dots [4,5]. To support this, wide variety of plant and other materials such as orange waste peels [19], corn flour [20], pure milk [21], *Syzygium cumini* [22], *Pyrus pyrifolia* [23], orange juice [24], dried shrimp [25], and low-cost organic chemicals [26,27] have been used as carbon sources for the synthesis of ultra-small fluorescent C-dots. These approaches have proved as green chemistry and exhibited attractive merits such as unique surface functionality with multicolor emissions, non-toxic and specific applications in sensing and in cell imaging.

Recently, various research groups have been explored the potential analytical applications of ultra-small C-dots by using various synthetic protocols. Briefly, Yang et al., synthesized C-dots from fungus for the detection of hyaluronic acid and hyaluronidase [28]. Ensafi's group derived ultra-small C-dots from the saffron and used as a probe for the detection of prilocaine with high selectivity and sensitivity [29]. A facile and cost-effective analytical strategy was developed for sensing of Fe^{3+} ion and imaging of cells by using C-dots derived from rose-heart radish [30]. Ansi and Renuka designed a simple and cost-effective

* Corresponding author.
E-mail addresses: skk@chem.svnit.ac.in, sureshkumarchem@gmail.com (S.K. Kailasa).

https://doi.org/10.1016/j.jphotobiol.2018.12.023
Received 4 October 2018; Received in revised form 24 December 2018; Accepted 27 December 2018
Available online 04 January 2019
1011-1344/

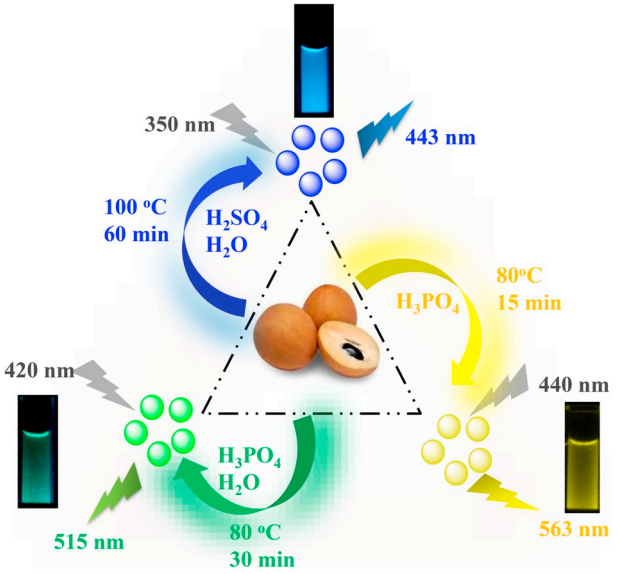

Scheme 1. Schematic procedure for the fabrication of blue-, green- and yellow-C-dots from *Manilkara zapota* fruits as a carbon source using H_2SO_4 and H_3PO_4 as oxidizing agents.

synthetic strategy for the fabrication of C-dots using table sugar as a precursor [31]. Apart from these, candle soot [32], chitosan gel [33], bovine serum albumin [34], lactose [35], glycerine [36], and single-walled carbon nanotubes [37] have been used as promising carbon sources for the synthesis of ultra-small C-dots for various applications.

In this work, a simple and green synthetic strategy that allows the fabrication of blue-, green-, and yellow- C-dots from *Manilkara zapota* (sapodilla) fruits using H_2SO_4 and H_3PO_4 as oxidizing agents. As shown in Scheme 1, multicolor (blue, green and yellow) C-dots were formed from *Manilkara zapota* fruits and existed with different surface functional groups, thus avoiding the tedious surface modifications. The synthesized C-dots are ultra-small size (1.9 ± 0.3, 2.9 ± 0.7and 4.5 ± 1.25 nm) and exhibited emission peaks at 443, 515 and 563 when excited at 350, 420 and 440 nm for blue-, green- and yellow- C-dots, respectively. The obtained three C-dots exhibit good QYs and non-toxic nature on HeLa cells. The C-dots have proven to be promising biocompatible fluorescent probes for imaging of *E. coli*, *Aspergillus aculeatus* and *Fomitopsis* sp. cells, suggesting the multi-color C-dots can be used as good candidates for biomedical applications.

2. Experimental Section

2.1. Materials

Manilkara zapota (local name- Chiku) fruits were purchased from local market, Surat, Gujarat, India. H_2SO_4 and H_3PO_4 were purchased from Finar PVT, LTD, India. Dialysis membrane-70 (molecular weight cut-off between 12 and 14 kDa) was procured from Hi-Media Laboratories Pvt., India. Milli-Q-purified water was utilized in all experiments.

2.2. Instrumentation

The absorption spectra were recorded by using Maya Pro 2000 spectrophotometer, Ocean Optics, USA, with 1 cm path length using quartz cuvette (light source: halogen and deuterium). Fluorescence excitation and emission spectra were measured by using Cary Eclipse fluorescence (Agilent Technologies, USA), with 5 nm slit width for both excitation and emission spectra using Xenon flash lamp. The surface chemistry of C-dots was measured by Fourier transform infrared (FT-IR) (Bruker, USA) spectrophotometer. The surface morphology and hydrodynamic average diameter of multicolor C-dots were characterized by high-resolution transmission electron microscopic (HR-TEM) (JEM-2100, JEOL, Japan) and dynamic light scattering (DLS) (Zetasizer Nano ZS90, Malvern, UK).

2.3. Quantum Yield Measurement

The QYs of blue-, green- and yellow- C-dots were determined by using quinine sulphate (0.1 M H_2SO_4) as a standard reference compound. The following equation was used to calculate QYs of three C-dots.

$$Q_{C-dots} = Q_R \cdot \frac{I_{C-dots}}{I_R} \cdot \frac{A_R}{A_{C-dots}} \cdot \frac{\eta^2_{C-dots}}{\eta^2_R}$$

where '*Q*' is the "QY", and "R" is the QY of reference compound. The '*I*' signifies the integrated fluorescent intensity and 'A' represents the absorbance and 'η' indicates the refractive index of the solvent. The subscript 'C-dots' stand for carbon dots.

2.4. Synthesis of Blue-, Green- and Yellow- C-Dots

Multi-color C-dots were synthesized by modifying the procedure in the literature [38]. *Manilkara zapota* fruits were washed thoroughly and peeled with stainless steel knife. The peeled fruits were chopped into small pieces and stored at −20 °C in a deep freezer. Then, 0.5 g of freeze dried *Manilkara zapota* fruit was taken into a 50 mL beaker that contains 5.0 mL of 34.0 N H_2SO_4. The mixture was sonicated for 5 min and then the solution was heated at 100 °C for 60 min. The obtained crude product pH was adjusted to pH 7.0 by treating with 2.0 M of NaOH. The solution was dialyzed against water for 24 h and the obtained blue C-dots were stored at 4 °C for future use.

The green C-dots were prepared by dissolving 0.5 g of freeze dried *Manilkara zapota* fruit in 10 mL of 40.0 N H_3PO_4 and 5 mL of water. The solution was heated at 80 °C for 30 min. The pH of the obtained residue was adjusted to pH 7.0 by neutralizing with 1.0 M of NaOH. The green C-dots were generated by dialysing the product with water for 24 h. Similarly, yellow C-dots were synthesized by dissolving 0.5 g of freeze dried *Manilkara zapota* fruit into 10 mL of 40.0 N H_3PO_4. The solution was heated at 80 °C for 15 min. The pH of the obtained crude was adjusted to pH 7.0 by neutralizing with 1.0 M of NaOH. The yellow C-dots were isolated by dialysing the product against water for 24 h. The obtained green and yellow C-dots were kept at 4 °C for further use.

2.5. Multi-color Imaging of E. coli, Aspergillus aculeatus and Fomitopsis sp. Cells Using Blue-, Green- and Yellow- C-dots

To confirm the cell imaging ability of three C-dots, *E. coli* (bacteria), *Aspergillus aculeatus* (fungi) and *Fomitopsis* sp. (fungi) cells were grown in Dulbecco's Modified Eagle's Medium (DMEM) with 1% penicillin streptomycin, 10% fetal bovine serum and 5% CO_2 as a medium and the cells were cultured at 37 °C. The *E. coli*, *Aspergillus aculeatus* and *Fomitopsis* sp. cells again subcultured and incubated with blue-, green- and yellow- C-dots (10 μg/mL) for 24 h, respectively. The *E. coli*, *Aspergillus aculeatus* and *Fomitopsis* sp. cells-C-dots were thoroughly washed with PBS three time and then the C-dots and *E. coli*, *Aspergillus aculeatus* and *Fomitopsis* sp. cells were fixed on imaging slide using 4% paraformaldehyde and 50% glycerol. The fluorescence images were captured by using confocal laser microscopy (Carl Zeiss 510 LSM, Jena, Germany). The blue, green and red fluorescence images were recorded by using laser excitation wavelengths at 405, 488 and 561 nm.

2.6. Cytotoxicity Studies

To evaluate the biocompatibility of three C-dots, methyl thiazolyl diphenyl-tetrazolium bromide (MTT) assay was evaluated on HeLa cells

to confirm the non-toxic nature of three C-dots. The HeLa cells were treated with blue-, green- and yellow- C-dots with different concentration (25, 50, 100, 200 and 300 µg/mL) and then kept for 15 h. The wells were washed with PBS (pH 7.4), each cell was treated with freshly prepared MTT (50 µL, 5 mg/mL) solution, and then incubated for 4 h. The MTT was removed from cell wells, and the wells were washed with PBS buffer for three times. Then, 150 µL of DMSO was added to each well and the absorbance of each well was recorded by Multimode microplate reader at 570 nm. The percentage of cell viability (%) was estimated by the ratio of absorbance of HeLa cells-C-dots to that of the control cells (without C-dots).

3. Results and Discussion

Manilkara zapota fruits contain various phytochemicals such as flavonoids, tannins, triterpenes, and saponins [39]. Further, the large amount of various carbohydrates was also present in the fruits of *Manilkara zapota*. These phytochemicals play significant role in generating ultra-small C-dots with multi-surface functional groups. To confirm this, blue-, green- and yellow- C-dots were fabricated by treating *Manilkara zapota* freeze dried fruits with H_2SO_4 at 100 °C (blue C-dots), and with H_3PO_4 at 80 °C for 30 and 15 min (Scheme 1). Fig. 1 shows the UV–visible absorption spectra of blue-, green- and yellow- C-dots derived from *Manilkara zapota* fruits. The absorption bands are located at 248, 395 and 489 nm for blue-, green- and yellow- C-dots and exhibited bright blue, green and yellow fluorescent colors under UV light irradiation at 365 nm (Insets of Fig. 1). These results revealed that the presence of electronic absorption transitions such as π-π* and n-π* transition, which confirms the existence of different surface states (C═C, C═N, C═O, and C−O) on the C-dots. Meanwhile, the strongest fluorescence emission wavelengths of blue-, green- and yellow- C-dots are 443, 515 and 563 nm when excited at 350, 420 and 440 nm, respectively (Fig. 1). The QYs of blue-, green- and yellow- C-dots are 5.7, 7.9 and 5.2%, respectively, which are higher than that of the reported methods [40,41].

The fluorescence emission spectra of three C-dots at different excitation wavelengths (300–400, 350–470 and 350–500 nm for blue-, green- and yellow- C-dots) revealed that the three C-dots exhibit excitation dependent emission properties (Supporting Information of Fig. S1). Thus, the fluorescence emission peaks were progressively red-shifted with increasing excitation wavelengths and the maximum emission peak intensities were observed at 443, 515 and 563 nm when excited at 350, 420 and 440 nm for blue-, green- and yellow- C-dots, respectively. These unique emission properties are due to the presence of different surface states, which are generated from multi-functional organic groups on the surfaces of C-dots and the slight variations in the sizes of C-dots [10]. The stability of blue-, green- and yellow- C-dots was studied by measuring emission spectra of three C-dots (Supporting Information of Fig. S2). It was noticed that the emission intensities of three C-dots were almost same upto 50 days after that the emission intensities of three C-dots were slightly decreased. The as-synthesized three C-dots were stable upto 100 days, which were quite enough for the bioimaging studies. The fluorescence lifetimes of blue-, green- and yellow- C-dots were shown in Supporting Information of Fig. S3. The average fluorescence lifetimes of blue-, green- and yellow- C-dots are found to be 4.9, 5.2 and 4.3 ns, confirming the life times of three C-dots are longer than the cell autofluorescence (< 6.0 ns) [42]. Thus, these features make them as promising fluorescent nanoprobes for cell imaging applications. The QYs of blue-, green- and yellow- C-dots were also measured at different excitation wavelengths in the range of 300–400 nm for blue C-dots, 350–470 nm for green C-dots and 350–500 nm for yellow C-dots, respectively (Supporting Information of Table. S1).

Surface chemistry of three C-dots derived from *Manilkara zapota* fruits was evaluated by FT-IR spectroscopy (Fig. 2). It can be noticed that the broad peaks at 3453, 3449 and 3451 cm^{-1} belong to the stretching vibrations of −OH groups of three C-dots. The stretching vibrations of −C═O and amide groups of three C-dots are noticed at 1635, 1642, and 1638 cm^{-1}, respectively. The peaks at (2826, 2853, 2988) and (1401,1400,1401) cm^{-1} are attributed to the stretching

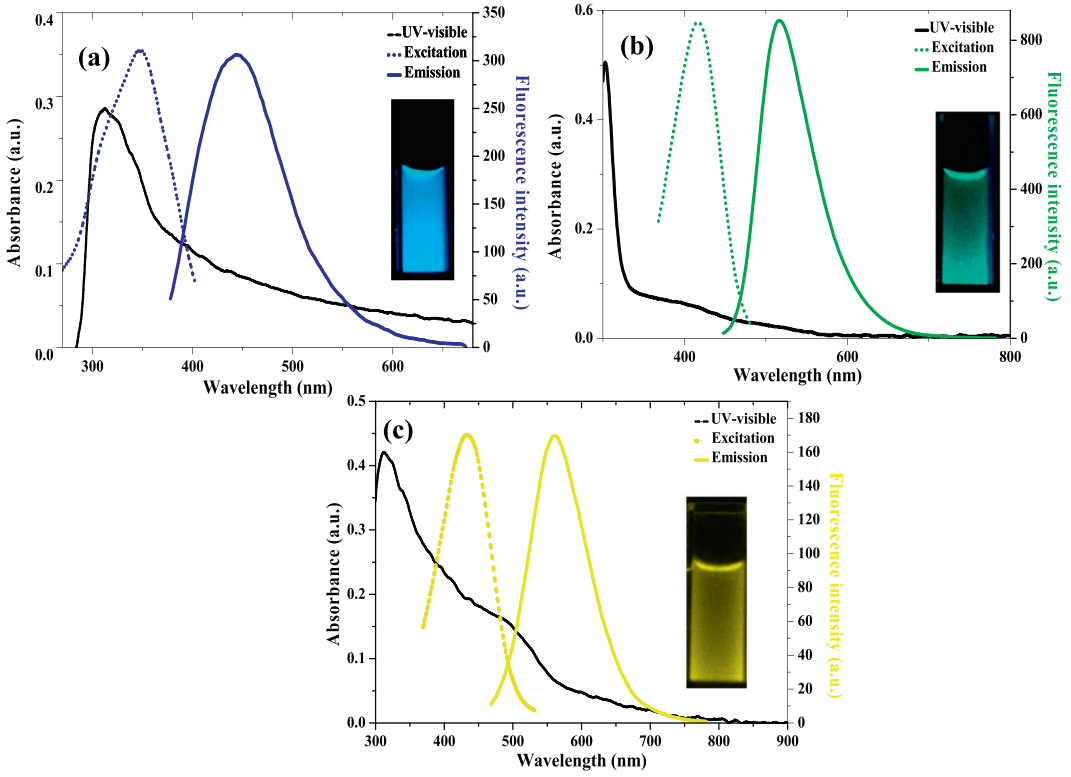

Fig. 1. UV–visible absorption and fluorescence (excitation and emission) spectra of (a) blue-, (b) green- and (c) yellow- C-dots derived from *Manilkara zapota* fruits.

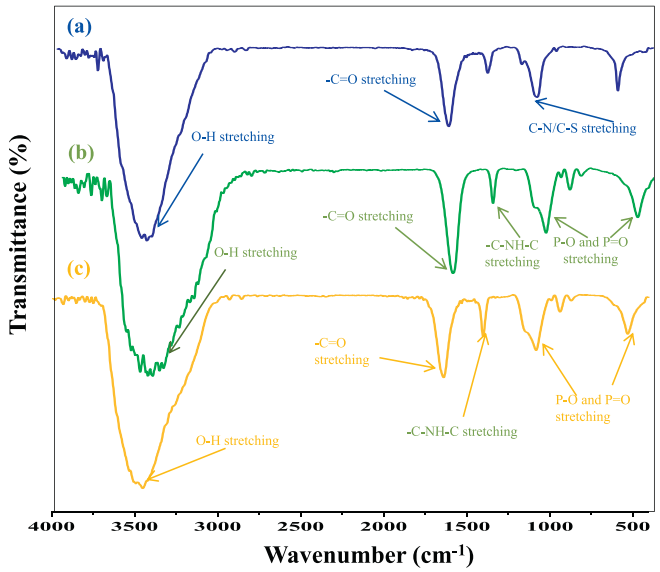

Fig. 2. FT-IR spectra of (a) blue-, (b) green- and (c) yellow- C-dots derived from *Manilkara zapota* fruits.

vibrations of −C−H, and −C−NH−C groups of blue-,green- and yellow C-dots, respectively. Similarly, C-N/C-S stretching vibrations were observed at 1195, 1143, 1142 cm^{-1}, respectively. The stretching vibrations of P−O and P═O groups of green- and yellow- C-dots were observed at (529,530), (937, 938) and (1082, 1081) cm^{-1}, respectively. These spectral characteristic strongly suggest that the formation of C-dots with multi-functional organic groups on the surfaces of C-dots.

The HR-TEM was studied to estimate the average sizes and morphologies of three C-dots (Fig. 3). The as-synthesized three C-dots are in spherical shape with uniform size distribution and the average sizes of blue-, green- and yellow- C-dots are to be 1.9 ± 0.3, 2.9 ± 0.7and 4.5 ± 1.25 nm, respectively. Moreover, the data of dynamic light scattering revealed that the mean hydrodynamic diameters of blue-, green- and yellow- C-dots are 7 ± 1.5, 8 ± 1.7 and 10 ± 2.1 nm, respectively (Supporting Information of Fig. S4), which are well consistent with the HR-TEM images of three C-dots. The HR-TEM images also revealed that the three C-dots are in crystalline structures, which confirms that the possessing of crystalline nature with graphitic carbon structures [22,23].

Further, X-ray photoelectron spectrometry (XPS) was studied to investigate the surface functional groups of three C-dots. As shown in Supporting Information of Fig. S5, the peaks at (143.9, 139. 9, 141.8), (296.6, 295.5, 297.1), (409.2, 406.6, 408.1), and (540.5, 535.8, 537.1) eV correspond to P 2p, C 1s, N 1s and O 1s of three C-dots, respectively, which signifies that the C-dots are composed of C, N, O, S and P elements. The high-resolution spectra of three C-dots of C 1s confirm the existence of C═C (286 and 287 for green and yellow C-dots), and C═O (288.42, 289.63, 289.18 eV) groups on the surfaces of three C-dots (Supporting Information of Fig. S6a). Similarly, the peaks at (399.28, 398.60, 397.98 eV), (400.66, 402.01, 402.59), (529.87 for blue-C-dots), (532.22 and 533.68 for green and yellow C-dots), and (537.93, 537.03, 538.43) eV are ascribed due to the presence of organic functional groups including N−H, C−N−C, C═O, C−O, and S-O/S-O onto the surfaces of three C-dots (Supporting Information of Fig. S6b-c). The peaks at (134.0, 136.09) eV belong to P−C group of green and yellow C-dots (Supporting Information of Fig. S6d). The sulfur-containing groups of blue C-dots such as C−S ($S2p_{3/2}$), C−S ($S2p_{1/2}$), and C−SO_x are observed at 162.0, 163.7, 166.5, 168.0, and 169.7 eV for blue C-dots, respectively (Supporting Information of Fig. S6e–f). These results suggest that the existence of multi-functional groups on the surfaces of three C-dots, which play significant role in tuning their optical properties.

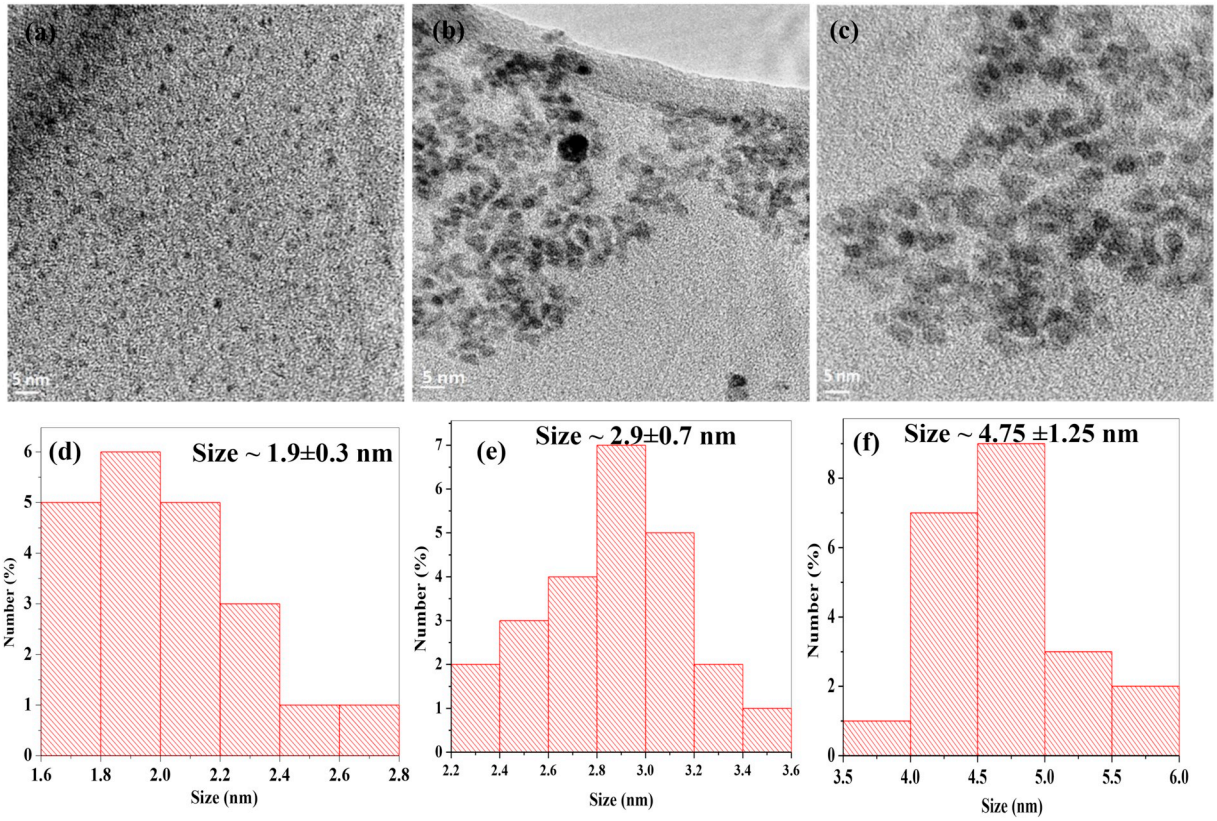

Fig. 3. HR-TEM images of (a) blue-, (b) green- and (c) yellow- C-dots derived from *Manilkara zapota* fruits. Histograms of (d) blue-, (e) green- and (f) yellow- C-dots at 5 nm scale bar.

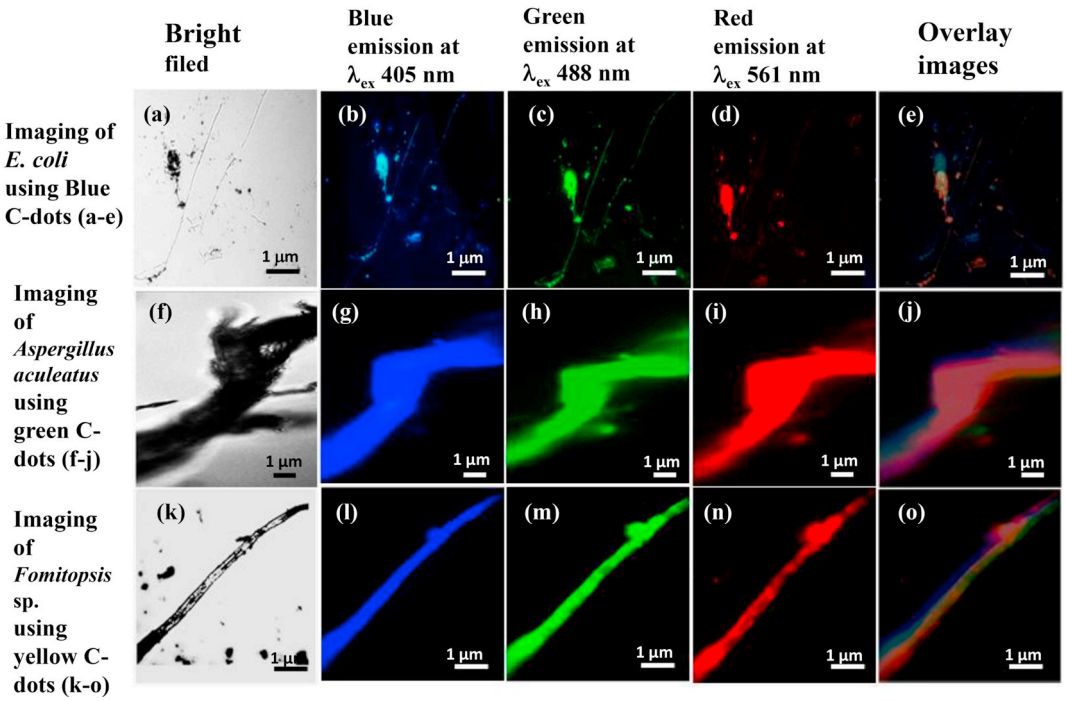

Fig. 4. Confocal fluorescence microscopic images of (a) *E. coli* (blue C-dots), (b) *Aspergillus aculeatus* (green C-dots) and (c) *Fomitopsis* sp. (yellow C-dots), at excitation wavelength of 405, 488 and 561 nm.

3.1. Imaging of E. coli, Aspergillus aculeatus and Fomitopsis sp. Cells and Cytotoxicity of HeLa Cells

Application of three C-dots in cell imaging was evaluated by using *E. coli* (bacteria), *Aspergillus aculeatus* (fungi) and *Fomitopsis* sp. (fungi) cells as a model. As shown in Fig. 4, three kinds (blue, green and yellow) of C-dots have provided blue, green and red color fluorescent signals at excitation wavelength 405, 488 and 561 nm with good intensity for cell imaging, and they are easily internalized into *E. coli*, *Aspergillus aculeatus* and *Fomitopsis* sp. cells via cell membrane through endocytosis. It can be noticed that the C-dots are located in the cell membrane as well as cytoplasm. Importantly, no obvious fluorescence signals are observed in the cells without C-dots, suggesting ultra-small C-dots are easily enter into the cells and high degree of distribution is observed, which leads to image cells with bright fluorescent signals. Further, the cytotoxicity of three C-dots are studied on HeLa cells, which confirm them as effective fluorescent probes for cell imaging. In this study, the cytotoxicity of three C-dots were evaluated on HeLa cells by MTT assay using different concentrations of blue-, green- and yellow- C-dots (25–300 μg/mL) (Supporting Information of Fig. S7). These results indicate that C-dots are exhibited non-toxicity upto 300 μg/mL, suggesting the three C-dots exhibited non-toxic nature to HeLa cells, which signifies that they can be used as good candidates for bioimaging applications.

3.2. Novelty and Significance of the Work

Various phytochemicals such as steroids, tannins, saponins, quinine, flavonoids, terpenoids, anthraquinine and carbohydrate were found in *Manilkara zapota* fruits. *Manilkara zapota* fruit can be strongly helpful in fighting against several inflammatory disorders, which is due to the presence of various phytochemicals, foliate, niacin acid and nutrients [39]. Because of these rich contents of various phytochemicals (flavonoids, carbohydrates, vitamins and minerals), *Manilkara zapota* fruit was used as a novel source for the synthesis of blue-, green- and yellow-C-dots. A simple and cost effective method was applied for the synthesis of multi-color (blue, green and yellow) fluorescent C-dots. The as-synthesized C-dots showed excitation dependent fluorescence behaviour with good QYs (5.7, 7.9 and 5.2% for blue-, green- and yellow- C-dots). Further, the as-synthesized blue-, green- and yellow- C-dots were highly stable up to 3 months. The as-fabricated blue-, green- and yellow C-dots exhibited good biocompatibility and non-toxic behaviour for bacterial, fungus and HeLa cells.

4. Conclusions

In this work, multi-color (blue, green and yellow) fluorescent C-dots are derived from *Manilkara zapota* fruits using H_2SO_4 and H_3PO_4 at different temperatures 100 and 80 °C for 60–15 min. The fabricated three C-dots are well dispersed with average sizes of 1.9 ± 0.3, 2.9 ± 0.7 and 4.5 ± 1.25 nm for blue-, green- and yellow- C-dots, respectively. The use of *Manilkara zapota* fruits as carbon source provides simple synthetic strategy for fabrication of C-dots with multi-color fluorescence emission and multi-functional organic groups on the surfaces of C-dots. The as-fabricated C-dots exhibited good QYs and excitation-dependent emission properties. As a result, they acted as promising agents for imaging of *E. coli*, *Aspergillus aculeatus* and *Fomitopsis* sp. cells with high degree of biocompatibility. Overall, the fabricated C-dots have proven to be potential agents for multi-color imaging of cells with high fluorescent signals, which allow them to use in bioimaging and optoelectronic applications.

Acknowledgments

This work was financial support by Department of Science and Technology, Government of India (EMR/2016/002621/IPC). JRB acknowledges the fellowship of Ph.D degree from the Director, SVNIT, Surat, India.

Appendix A. Supplementary data

Supplementary data to this article can be found online at https://doi.org/10.1016/j.jphotobiol.2018.12.023.

References

[1] M. Tuerhong, Y. Xu, X.-B. Yin, Review on carbon dots and their applications, Chin. J. Anal. Chem. 45 (2017) 139–150.

[2] L. Lin, M. Rong, F. Luo, D. Chen, Y. Wang, X. Chen, Luminescent graphene quantum dots as new fluorescent materials for environmental and biological applications, TrAC Trends Anal. Chem. 54 (2014) 83–102.

[3] C.W. Lai, Y.H. Hsiao, Y.K. Peng, P.T. Chou, Facile synthesis of highly emissive carbon dots from pyrolysis of glycerol; gram scale production of carbon dots/$mSiO_2$ for cell imaging and drug release, J. Mater. Chem. 22 (2012) 14403–14409.

[4] Y. Choi, S. Kim, M.H. Choi, S.R. Ryoo, J. Park, D.H. Min, B.S. Kim, Highly biocompatible carbon nanodots for simultaneous bioimaging and targeted photodynamic therapy *in vitro* and *in vivo*, Adv. Funct. Mater. 24 (2014) 5781–5789.

[5] S.T. Yang, L. Cao, P.G. Luo, F. Lu, X. Wang, H. Wang, M.J. Meziani, Y. Liu, G. Qi, Y.P. Sun, Carbon dots for optical imaging *in vivo*, J. Am. Chem. Soc. 131 (2009) 11308–11309.

[6] P.G. Luo, S. Sahu, S.T. Yang, S.K. Sonkar, J. Wang, H. Wang, G.E. LeCroy, L. Cao, Y.P. Sun, Carbon "quantum" dots for optical bioimaging, J. Mater. Chem. B 1 (2013) 2116–2127.

[7] J. Shen, Y. Zhu, X. Yang, C. Li, Graphene quantum dots: emergent nanolights for bioimaging, sensors, catalysis and photovoltaic devices, Chem. Commun. 48 (2012) 3686–3699.

[8] L. Li, G. Wu, G. Yang, J. Peng, J. Zhao, J.-J. Zhu, Focusing on luminescent graphene quantum dots: current status and future perspectives, Nanoscale 5 (2013) 4015–4039.

[9] Z. Zhang, J. Zhang, N. Chen, L. Qu, Graphene quantum dots: an emerging material for energy-related applications and beyond, Energy Environ. Sci. 5 (2012) 8869–8890.

[10] Y.P. Sun, B. Zhou, Y. Lin, W. Wang, K.A.S. Fernando, P. Pathak, M.J. Meziani, B.A. Harruff, X. Wang, H. Wang, P.G. Luo, H. Yang, M.E. Kose, B. Chen, L.M. Veca, S.Y. Xie, Quantum-sized carbon dots for bright and colorful photoluminescence, J. Am. Chem. Soc. 128 (2006) 7756–7757.

[11] L. Cao, X. Wang, M.J. Meziani, F. Lu, H. Wang, P.G. Luo, Y. Lin, B.A. Harruff, L.M. Veca, D. Murray, S.Y. Xie, Y.P. Sun, Carbon dots for multiphoton bioimaging, J. Am. Chem. Soc. 129 (2007) 11318–11319.

[12] X. Xu, R. Ray, Y. Gu, H.J. Ploehn, L. Gearheart, K. Raker, W.A. Scrivens, Electrophoretic analysis and purification of fluorescent single-walled carbon nanotube fragments, J. Am. Chem. Soc. 126 (2004) 12736–12737.

[13] J.R. Bhamore, S. Jha, T.J. Park, S.K. Kailasa, Fluorescence sensing of Cu^{2+} ion and imaging of fungal cell by ultra-small fluorescent carbon dots derived from *Acacia concinna* seeds, Sensors Actuators B Chem. 277 (2018) 47–54.

[14] S. Liu, J. Tian, L. Wang, Y. Luo, X. Sun, A general strategy for the production of photoluminescent carbon nitride dots from organic amines and their application as novel peroxidase-like catalysts for colorimetric detection of H_2O_2 and glucose, RSC Adv. 2 (2012) 411–413.

[15] W. Wang, Y. Li, L. Cheng, Z. Cao, W. Liu, Water-soluble and phosphorus-containing carbon dots with strong green fluorescence for cell labelling, J. Mater. Chem. B 2 (2014) 46–48.

[16] L. Shi, X. Li, Y. Li, X. Wen, J. Li, M.M.F. Choi, C. Dong, S. Shuang, Naked oats-derived dual-emission carbon nanodots for ratiometric sensing and cellular imaging, Sensors Actuators B Chem. 210 (2015) 533–541.

[17] N. Gong, H. Wang, S. Li, Y. Deng, X. Chen, L. Ye, W. Gu, Microwave-assisted polyol synthesis of gadolinium-doped green luminescent carbon dots as a bimodal nanoprobe, Langmuir 30 (2014) 10933–10939.

[18] C.L. Li, C.M. Ou, C.C. Huang, W.C. Wu, Y.P. Chen, T.E. Lin, L.C. Ho, C.W. Wang, C.C. Shih, H.C. Zhou, Y.C. Lee, W.F. Tzeng, T.J. Chiou, S.T. Chu, J. Cang, H.T. Chang, Carbon dots prepared from ginger exhibiting efficient inhibition of human hepatocellular carcinoma cells, J. Mater. Chem. B 2 (2014) 4564–4571.

[19] A. Prasannan, T. Imae, One-pot synthesis of fluorescent carbon dots from orange waste peels, Ind. Eng. Chem. Res. 52 (2013) 15673–15678.

[20] J. Wei, X. Zhang, Y. Sheng, J. Shen, P. Huang, S. Guo, J. Pan, B. Feng, Dual functional carbon dots derived from cornflour *via* a simple one-pot hydrothermal route, Mater. Lett. 123 (2014) 107–111.

[21] D. Wang, X. Wang, Y. Guo, W. Liu, W. Qin, Luminescent properties of milk carbon dots and their sulphur and nitrogen doped analogues, RSC Adv. 4 (2014) 51658–51665.

[22] J.R. Bhamore, S. Jha, R.K. Singhal, S.K. Kailasa, Synthesis of water dispersible fluorescent carbon nanocrystals from *Syzygium cumini* fruits for the detection of Fe^{3+} ion in water and biological samples and imaging of *Fusarium avenaceum* cells, J. Fluoresc. 27 (2017) 125–134.

[23] J.R. Bhamore, S. Jha, R.K. Singhal, T.J. Park, S.K. Kailasa, Facile green synthesis of carbon dots from *Pyrus pyrifolia* fruit for assaying of Al^{3+} ion via chelation enhanced fluorescence mechanism, J. Mol. Liq. 264 (2018) 9–16.

[24] S. Sahu, B. Behera, T.K. Maitib, S. Mohapatra, Simple one-step synthesis of highly luminescent carbon dots from orange juice: application as excellent bio-imaging agents, Chem. Commun. 48 (2012) 8835–8837.

[25] S.L. D'souza, B. Deshmukh, J.R. Bhamore, K.A. Rawat, N. Lenka, S.K. Kailasa, Synthesis of fluorescent nitrogen-doped carbon dots from dried shrimps for cell imaging and boldine drug delivery system, RSC Adv. 6 (2016) 12169–12179.

[26] X. Li, H. Wang, Y. Shimizu, A. Pyatenko, K. Kawaguchi, N. Koshizaki, Preparation of carbon quantum dots with tunable photoluminescence by rapid laser passivation in ordinary organic solvents, Chem. Commun. 47 (2011) 932–934.

[27] P.C. Hsu, H.T. Chang, Synthesis of high-quality carbon nanodots from hydrophilic compounds: role of functional groups, Chem. Commun. 48 (2012) 3984–3986.

[28] K. Yang, M. Liu, Y. Wang, S. Wang, H. Miao, L. Yang, X. Yang, Carbon dots derived from fungus for sensing hyaluronic acid and hyaluronidase, Sensors Actuators B Chem. 251 (2017) 503–508.

[29] A.A. Ensafi, S. Hghighat Sefat, N. Kazemifard, B. Rezaei, F. Moradi, A novel one-step and green synthesis of highly fluorescent carbon dots from saffron for cell imaging and sensing of prilocaine, Sensors Actuators B Chem. 253 (2017) 451–460.

[30] W. Liu, H. Diao, H. Chang, H. Wang, T. Li, W. Wei, Green synthesis of carbon dots from rose-heart radish and application for Fe^{3+} detection and cell imaging, Sensors Actuators B Chem. 241 (2017) 190–198.

[31] V.A. Ansi, N.K. Renuka, Table sugar derived Carbon dot – a naked eye sensor for toxic Pb^{2+} ions, Sensors Actuators B Chem. 264 (2018) 67–75.

[32] L.L. Qin, L.Y. Fang, Z. Lei, L. Yue, H.C. Zhi, One-step synthesis of fluorescent hydroxyls-coated carbon dots with hydrothermal reaction and its application to optical sensing of metal ions, Sci. China Chem. 54 (2011) 1342–1347.

[33] X. Gong, Q. Hu, M.C. Paau, Y. Zhang, L. Zhang, S. Shuang, C. Dong, M.M.F. Choi, High-performance liquid chromatographic and mass spectrometric analysis of fluorescent carbon nanodots, Talanta 129 (2014) 529–538.

[34] Z. Zhang, J. Hao, J. Zhang, B. Zhang, J. Tang, Protein as the source for synthesizing fluorescent carbon dots by a one-pot hydrothermal route, RSC Adv. 2 (2012) 8599–8601.

[35] Y.Y. Zhang, M. Wu, Y.Q. Wang, X.W. He, W.Y. Li, X.Z. Feng, A new hydrothermal refluxing route to strong fluorescent carbon dots and its application as fluorescent imaging agent, Talanta 117 (2013) 196–202.

[36] M. Amjadi, J.L. Manzoori, T. Hallaj, A novel chemiluminescence method for determination of bisphenol A based on the carbon dot-enhanced HCO_3^-–H_2O_2 system, J. Lumin. 158 (2015) 160–164.

[37] H. Ding, L.-W. Cheng, Y.-Y. Ma, J.-L. Kong, H.-M. Xiong, Luminescent carbon quantum dots and their application in cell imaging, New J. Chem. 37 (2013) 2515–2520.

[38] C.J. Jeong, A.K. Roy, S.H. Kim, J.-E. Lee, J.H. Jeong, I. In, S.Y. Park, Fluorescent carbon nanoparticles derived from natural materials of mango fruit for bio-imaging probes, Nanoscale 6 (2014) 15196–15202.

[39] A. Jenitha, M. Bhuvaneshwari, In vitro studies on phytochemical analysis and antioxidant activity of *Manilkara zapota*, Int. J. Res. Pharmacol. Pharmacother. 5 (2016) 153–161.

[40] X. Qin, W. Lu, A.M. Asiri, A.O. Al-Youbi, X. Sun, Microwave-assisted rapid green synthesis of photoluminescent carbon nanodots from flour and their applications for sensitive and selective detection of mercury(II) ions, Sensors Actuators B Chem. 184 (2013) 156–162.

[41] A. Mewada, S. Pandey, S. Shinde, N. Mishra, G. Oza, M. Thakur, M. Sharon, Green synthesis of biocompatible carbon dots using aqueous extract of *Trapa bispinosa* peel, Mater. Sci. Eng. C 33 (2013) 2914–2917.

[42] U. Resch-Genger, M. Grabolle, S. Cavaliere-Jaricot, R. Nitschke, T. Nann, Quantum dots versus organic dyes as fluorescent labels, Nat. Methods 5 (2008) 763–775.